International Journal of Applied Pharmaceutics

ISSN- 0975-7058 Vol 18, Issue 3, 2026

Original Article

DESIGN, OPTIMIZATION, AND EVALUATION OF A LORNOXICAM-LOADED TRANSETHOSOMAL GEL FOR ENHANCED TRANSDERMAL DELIVERY

NABAMITA SEN[1,2*], FOWAD KHURSHID[3], M. GANGA RAJU[4]

[1]Department of Pharmacy, Institute of Biomedical Education and Research, Mangalayatan University, Aligarh, (U. P), India. [2]Gokaraju Rangaraju College of Pharmacy, Bachupally, Hyderabad-500090, Telangana, India. [3]Department of Pharmacy, Institute of Biomedical Education and Research, Mangalayatan University, Aligarh-202146, India. [4]Gokaraju Rangaraju College of Pharmacy, Bachupally, Hyderabad-500090, Telangana, India

*Corresponding author: Nabamita Sen; *Email: nabamitas961@gmail.com

Received: 29 Dec 2025, Revised and Accepted: 25 Feb 2026

ABSTRACT

Objective: Lornoxicam is an effective oxicam-class non-steroidal anti-inflammatory agent administered in the managing acute and chronic inflammatory conditions. However, its oral administration is inadequate by deprived aqueous solubility, extensive first-pass metabolism, and gastrointestinal adverse effects. Transdermal drug delivery offers a promising alternative by bypassing hepatic metabolism and enabling sustained drug release, although the stratum corneum restricts effective drug permeation. Transethosomes, ultradeformable vesicular carriers, have shown considerable potential in enhancing transdermal drug transport.

Methods: Lornoxicam-loaded transethosomes were obtained by the cold method and optimized by3-factor, 3-level Box–Behnken design. Phospholipid (soya lecithin), surfactant (Tween 80), and ethanol concentrations selected as independent attributes, vesicle size and entrapment efficiency (EE) evaluated as critical responses. Optimized composition fused intoCarbopol-934 gel base and characterized for physicochemical properties, vesicle morphology, zeta potential, *in vitro* drug release, *in vitro* permeation, and short-term stability.

Results: Optimization studies demonstrated that phospholipid and surfactant concentrations majorly impacted vesicle size and %EE, whereas ethanol played huge role in enhancing membrane fluidity and permeation. The optimized formulation (LRNX-12) exhibited nanosized vesicles (179 nm), improved (81.8%), and a favorable negative zeta potential (−34.6 mV), indicating good stability. Transmission Electron Microscopy analysis confirmed spherical vesicles with smooth morphology consistent with entrapment. The release data were fitted to zero-order, first-order, Higuchi, and Korsmeyer–Peppas models. The highest correlation coefficient was obtained for the Higuchi model (R^2 = 0.97), indicating diffusion-controlled release. *In vitro* permeation studies showed significantly higher drug permeation from the transethosomal gel (93% at 24 h) compared with the conventional plain gel (45%). The gel showed acceptable pH, viscosity, spreadability, and good stability.

Conclusion: The lornoxicam-loaded transethosomal gel demonstrated enhanced transdermal delivery with sustained release and superior permeation, offering a promising alternative to oral therapy for inflammatory conditions.

Keywords: Lornoxicam, Transethosomes, Transdermal drug delivery, Box–behnken design, Vesicular gel

DOI: https://dx.doi.org/10.22159/ijap.2026v18i3.57942 Journal homepage: https://innovareacademics.in/journals/index.php/ijap

INTRODUCTION

Lornoxicam is a potent non-steroidal anti-inflammatory drug (NSAID) of oxicam class that is broadly administered for managing acute and chronic inflammatory conditions, like osteoarthritis, rheumatoid arthritis, postoperative pain, and musculoskeletal disorders [1]. Since its clinical evaluation, lornoxicam has gained attention due to its strong analgesic and anti-inflammatory activity at relatively low doses. Its pharmacological action is primarily mediated through non-selective inhibition of cyclooxygenase (COX-1 and COX-2) enzymes, ensuing in reduced synthesis of prostaglandins responsible for pain, inflammation, and edema [2]. Additional modulation of inflammatory mediators such as nitric oxide further contributes to its therapeutic efficacy [3]. Despite these advantages, the clinical utility of lornoxicam following oral administration is significantly limited by formulation and pharmacokinetic challenges [4]. The drug exhibits low water solubility and dissolution-rate limited absorption, causing variable and often inadequate systemic absorption [5]. Moreover, lornoxicam undergoes extensive first-pass hepatic metabolism, predominantly via CYP2C9, which markedly reduces its oral bioavailability [4]. These limitations necessitate frequent dosing, increasing the risk of NSAID-associated adverse effects such as gastrointestinal irritation, ulceration, renal toxicity, and cardiovascular complications [6]. Consequently, long-term oral therapy is particularly problematic in elderly patients and those with comorbidities, underscoring the need for alternative delivery strategies that can improve safety and therapeutic consistency [7].

Transdermal drug delivery offers a compelling substitute to oral NSAIDs by evading first-pass metabolism, reducing gastrointestinal exposure, and enabling sustained drug release [8]. Clinically successful transdermal NSAID products, including diclofenac, ketoprofen, and piroxicam gels and patches, validate the feasibility of this route for inflammatory pain management [9]. However, the stratum corneum remains a major barrier to drug permeation, particularly for molecules such as lornoxicam that possess suboptimal physicochemical properties for passive diffusion [10]. Conventional topical formulations therefore often fail to deliver therapeutically effective drug concentrations across the skin [11]. To overcome these challenges, several novel formulation strategies have been explored for lornoxicam, including solid dispersions, cyclodextrin complexes, nanosuspensions, lipid-based systems, and polymeric nanoparticles. While these approaches have shown improvements in solubility and dissolution, many remain limited by stability issues, manufacturing complexity, or continued reliance on oral administration [12]. In contrast, vesicular nanocarriers have developed as a capable platform for transdermal drug delivery because of ability to interact with skin lipids and facilitate deeper penetration [13].

Transethosomes, an advanced class of ultradeformable vesicles composed of phospholipids, ethanol, and surfactants, have demonstrated superior skin permeation compared with conventional liposomes and ethosomes [14]. Ethanol enhances vesicle flexibility and disrupts stratum corneum lipid organization, while surfactants impart elasticity, enabling efficient transport through narrow intercellular pathways [15]. When incorporated into a gel base, transethosomal systems offer additional advantages such as prolonged skin residence time, controlled drug release, improved

stability, and enhanced patient compliance [16]. Although nano-vesicular transdermal formulations of several NSAIDs have shown promising outcomes, commercially available lornoxicam transdermal products remain limited, highlighting a significant opportunity for innovation [17].

The novelty of the present work lies in the systematic design, optimization, and evaluation of a lornoxicam-loaded transethosomal gel using a Box–Behnken experimental design to precisely elucidate the influence of formulation variables on vesicle size and entrapment efficiency. Furthermore, incorporation of the optimized transethosomes into a Carbopol gel matrix was strategically employed to enhance formulation stability, prolong skin residence time, and achieve sustained transdermal delivery. This combined approach addresses the limitations of existing lornoxicam delivery systems and provides a scientifically robust and clinically relevant alternative to conventional oral and topical therapies.

The current study aims to develop and optimize a lornoxicam-oriented transethosomal gel for transdermal delivery to overcome the limitations of oral therapy. The objectives include formulation and optimization of transethosomal vesicles, physicochemical and morphological characterization, evaluation of *in vitro* drug release and permeation, incorporation into a suitable gel matrix, and assessment of formulation stability. This approach is expected to enhance transdermal delivery efficiency, improve anti-inflammatory efficacy, and reduce systemic adverse effects, thereby offering a clinically relevant and high-impact alternative for lornoxicam therapy.

MATERIALS AND METHODS

Materials

Lornoxicam was an attained gift sample from Hetero Drugs Ltd., Hyderabad, India. Soya lecithin was procured from Bright Laboratories, India. Tween 80 was acquired from Merck Specialties Pvt. Ltd., India. Ethanol, Carbopol 934, triethanolamine, and other analytical grade reagents were sourced from Merck India Pvt. Ltd. Ultrapure water (Milli-Q grade) was used throughout study. All chemicals and solvents employed were of analytical grade and were used as received with no further purification.

Methods

Compatibility studies

Compatibility among lornoxicam and the designated excipients was evaluated by means of Fourier transform infrared (FTIR) spectroscopy (Bruker Alpha-T-1020, Germany). Potassium bromide (KBr) pellets were prepared by intimately mixing lornoxicam or its physical mixtures with excipients with dry KBr in a 1:100 (w/w) ratio, followed by compression in a stainless-steel die at a pressure of approximately 8 t/in^2. The FTIR spectra were recorded in wavenumber range of 3500–500 cm^{-1}. Spectra were analyzed for presence, shifting, or disappearance of characteristic absorption bands of lornoxicam to identify any possible drug–excipient interactions [18].

Preparation of lornoxicam-loaded transethosomes

Lornoxicam-loaded transethosomes (LRNX1–LRNX14) were prepared by the cold method, which is commonly employed for the fabrication of ethosomal and transethosomal vesicular systems due to its simplicity and suitability for thermolabile drugs. Briefly, accurately weighed quantities of phospholipid (Soyalecithin, up to1.3% w/v) and surfactant (Tween 80, 0.5–1.5% w/v) were dissolved in ethanol (10–35% v/v) in a closed glass vial and maintained at 30±1 °C using a thermostatically controlled water bath. Lornoxicam (0.1–0.3% w/v) was then added to this ethanolic lipid phase and magnetically stirred until a clear and homogeneous solution was obtained, ensuring complete solubilization of the drug [19].

In parallel, ultrapure water was heated separately to the same temperature (30±1 °C) and maintained under continuous magnetic stirring to serve as aqueous phase. Aqueous phase then placed dropwise to organic phase at a controlled rate under constant stirring at 700 rpm. Upon addition, spontaneous formation of nanosized vesicles occurred due to the ethanol–water transition and self-assembly of phospholipids into flexible bilayers. The dispersion was further stirred for 30 min to ensure complete vesicle formation and uniformity of the system, as reported in earlier transethosomal formulation studies [20].

The freshly prepared transethosomal dispersion was subsequently stored at 4 °C for 24 hr to let vesicle maturation, stabilization, and equilibration of the lipid bilayers. Following this maturation period, the dispersion was exposed to probe sonication (Sonics Vibra-Cell, USA) for 3–5 min at with 30-s cooling intervals, 40% amplitude with intermittent pulses to reduce vesicle size and achieve a narrow size distribution while avoiding excessive thermal stress. All formulations contained 80 mg lornoxicam per 100 ml final volume. The final volume was adjusted to 100 ml using distilled water. The optimized lornoxicam-loaded transethosomal formulations were transferred into amber-coloured glass vials to protect them from light and stored at 4 °C until further physicochemical characterization and evaluation (table 1).

Table 1: Composition of Lornoxicam-loaded formulations. All quantities are expressed per 100 ml final volume; the final volume of each formulation was adjusted to 100 ml with distilled water

Formulation	Lecithin	Lornoxicam	Ethanol	Tween 80
LRNX 1	90 mg	80 mg	15 ml	10 ml
LRNX2	110 mg	80 mg	15 ml	10 ml
LRNX3	130 mg	80 mg	10 ml	10 ml
LRNX 4	90 mg	80 mg	10 ml	10 ml
LRNX 5	110 mg	80 mg	20 ml	15 ml
LRNX 6	130 mg	80 mg	15 ml	10 ml
LRNX 7	90 mg	80 mg	15 ml	15 ml
LRNX 8	110 mg	80 mg	15 ml	15 ml
LRNX 9	130 mg	80 mg	20 ml	10 ml
LRNX 10	90 mg	80 mg	10 ml	5 ml
LRNX 11	110 mg	80 mg	20 ml	5 ml
LRNX 12	130 mg	80 mg	20 ml	10 ml
LRNX 13	90 mg	80 mg	10 ml	15 ml
LRNX 14	110 mg	80 mg	15 ml	5 ml

Optimization

Optimization of lornoxicam-loaded transethosomal formulations was performed by response surface methodology (RSM) method reliant on the Box–Behnken design (BBD). On basis of an extensive review of previously reported ethosomal and transethosomal systems, three formulation variables known to critically influence vesicle characteristics and transdermal performance were selected as independent factors. These included phospholipid concentrations (X_1), ethanol concentration (X_2), and surfactant concentration (Tween 80; X_3). Each feature was evaluated at three levels (low, medium, and high) to systematically study both individual and interactive impacts on formulation performance [21-23].

A 3-factor, 3-level BBD consisting of 14 runs, counting five centre-point replicates, was generated by Design-Expert® software (Version 7.1.6, Stat-Ease Inc. and Minneapolis, USA). Inclusion of multiple centre points enabled estimation of experimental error and ensured the robustness, reproducibility, and statistical validity of the developed quadratic model. The selected dependent response variables were particle size (Y_1) and entrapment efficiency (EE; Y_2), as these parameters are critical determinants of skin permeation, stability, and therapeutic efficacy of transdermal vesicular systems.

The experimental data obtained from the 14 formulation runs were tailored to a 2nd-order polynomial equation to define relationship among independent attributes and measured results. Response surface and contour charts were created to envision influence of formulation attributes and their interactions on vesicle size and EE. Analysis of variance (ANOVA) evaluated significance of model, regression coefficients, and interaction terms at a confidence level of 95%. The optimized formulation selected relying on desirability principles aimed at achieving least vesicle size and maximum drug EE.

The coded and actual levels of the independent attributes used in BBD are summarized in table 2, while the corresponding vesicle size and EE values obtained for each formulation are presented in Tables 2 and 3, respectively. All formulation variables were expressed as concentrations (% w/v or % v/v) relative to a final volume of 100 ml to ensure experimental reproducibility, regulatory relevance, and meaningful interpretation of factor effects.

Table 2: Independent dependent attributes for transethosomes formulation. All quantities are expressed per 100 ml final volume; the final volume of each formulation was adjusted to 100 ml with distilled water

Independent attributes			**Level**		
Attribute	**Details**	**Units**	**Low (-1)**	**Middle (0)**	**High (+1)**
A	Lecithin amount	% w/v	0.90	1.10	1.30
B	Ethanol amount	% v/v	10	15	20
C	Tween 80amount	% v/v	0.5	1.0	1.5
Dependent variable			Goal		
Y1	Particle size		nm	Minimize	
Y2	Entrapment efficiency of lornoxicam		%	Maximize	

Table 3: Optimizing within dependent features and outcomes of dependent attributes. All quantities are expressed per 100 ml final volume; the final volume of each formulation was adjusted to 100 ml with distilled water

Std	**Run**	**Factor 1**	**Factor 2**	**Factor 3**	**Response 1**	**Response 2**
		A: Soya lecithin (% w/v)	**B: Ethanol (% v/v)**	**C: Tween 80 (% v/v)**	**Vesicle size (nm)**	**% EE**
15	1	1.10	15	1.0	150.8±6.7	73.8±8.1
13	2	1.10	15	1.0	152.6±5.1	73.5±6.9
2	3	1.30	10	1.0	210.6±7.9	74.8±7.0
1	4	0.90	10	1.0	182.4±5.9	61.2±4.8
12	5	1.10	20	1.5	136.9±5.0	71.8±7.0
4	6	1.30	20	1.0	198.9±6.3	78.6±6.1
8	7	1.30	15	1.5	164.2±7.7	72.5± 7.3
7	8	0.90	15	1.5	138.6 ±7.1	59.8 ±8.2
3	9	0.90	20	1.0	156.3±8.3	65.7±8.0
9	10	1.10	10	0.5	187.0±6.0	70.3±5.9
10	11	1.10	20	0.5	161.2±2.9	74.6±7.0
14	12	1.10	15	1.0	151.9±7.3	72.9±6.5
11	13	1.10	10	1.5	149.7±2.7	66.2±6.2
5	14	0.90	15	0.5	158.7±3.7	63.4±4.4
17	15	1.10	15	1.0	151.2±7.0	73.2±3.9
16	16	1.10	15	1.0	149.6±4.9	74.1±0.9
6	17	1.30	15	0.5	203.5±8.1	76.9±6.9

All values are articulated as mean±SD (n = 3)

Evaluation of lornoxicam-loaded transethosomes

Particle size, zeta potential and polydispersity index

Vesicle size and polydispersity index (PDI) of lornoxicam-transethosomal formulations (LRNX1–LRNX14) were measured by a laser light scattering-particle size analyzer (HORIBA PS-100, Japan). Prior to analysis, 1 ml of each transethosomal dispersion was suitably diluted tenfold with distilled water to avoid multiple scattering effects and to ensure accurate measurement. The samples were gently mixed to maintain vesicle integrity and analyzed at room temperature. Particle size was expressed as Z-average (Z-mean), which represents intensity-weighted mean hydrodynamic diameter of vesicles. The PDI, a dimensionless parameter indicative of vesicle size distribution and homogeneity, was also recorded. Lower PDI values indicate slender and uniform size dispersal, which is required for stable and reproducible transdermal vesicular systems [24]. In addition, zeta potential (measured in distilled water) of optimized lornoxicam-loaded transethosomal formulation measured using same instrument to assess surface charge and colloidal stability. The zeta potential value provides insight into electrostatic repulsion between vesicles, with higher absolute values indicating improved physical stability of the transethosomal dispersion.

Differential scanning calorimetry (DSC)

Thermal investigation of lornoxicam, individual excipients, the physical mixture, and the lornoxicam-loaded transethosomal formulation was supported using differential scanning calorimeter. Accurately weighed samples (approximately 3–5 mg) placed in standard aluminum pans and hermetically sealed, with an empty pan as reference. Samples heated over a temperature range of 30 to 400 °C at a constant rate of 10 °C per min at constant nitrogen purge to prevent oxidative degradation. Resulting thermograms recorded and analyzed to identify characteristic thermal transitions, such as melting endotherms, glass transition events, and changes in peak intensity or position. Comparison of the thermograms of pure drug, excipients, physical mix, and drug-transethosomes was performed to assess the crystalline or amorphous nature of lornoxicam and to evaluate possible drug–excipient interactions and thermal compatibility within the formulation.

Transmission electron microscopy (TEM)

The morphological characteristics of optimized lornoxicam-loaded transethosomal formulation were examined by transmission electron microscopy. A small aliquot of the freshly prepared transethosomal dispersion was suitably diluted with water to get an appropriate particle concentration. A drop of diluted sample was located onto carbon-coated copper grid and permitted to stand for a short period to facilitate adsorption of the vesicles onto the grid surface. Extra liquid was cautiously removed by filter paper, and sample negatively stained with a suitable contrast-enhancing agent to improve image clarity. The grids were then air-dried at room temperature and inspected under transmission electron microscope operated at an appropriate accelerating voltage. TEM images were captured at different magnifications, corresponding to 200 nm and 500 nm scales, to assess shape, size, surface characteristics, and aggregation behavior of transethosomal formulation.

Entrapment efficiency (EE)

EE was within transethosomal vesicles was measured using an indirect high-speed centrifugation method. Briefly, an accurately measured volume (10 ml) of each transethosomal formulation (LRNX1–LRNX14) was subjected to high-speed centrifugation at 12,000rpm for 30 min by a refrigerated centrifuge (C-24, Remi Instruments, India) to separate the unentrapped (free) drug from the vesicular fraction. Following centrifugation, the clear supernatant containing the unentrapped lornoxicam was cautiously collected without distressing vesicle pellet [25]. Concentration of free drug in supernatant quantified by UV–Visible spectrophotometer (Shimadzu, Japan) at wavelength (λ_max) of 376 nm against an appropriate blank. Drug concentrations were calculated by a before constructed calibration plot, which exhibited good linearity (R^2 = 0.9952). The EE (%) of lornoxicam was calculated using following equation:

$$\text{EE (\%)} = \frac{\text{Total amount of drug} - \text{Amount of free drug}}{\text{Total amount of drug}} \text{X } 100$$

This method provides an accurate estimation of drug entrapment within transethosomal vesicles and is widely employed for evaluating vesicular drug delivery systems.

***In vitro* drug release from transethosomes**

The *in vitro* drug release behavior of the optimized lornoxicam-transethosomal formulation (LRNX12) evaluated by a suitable diffusion method to assess release profile over 24 h. A precisely measured quantity of formulation, equivalent to a known amount of lornoxicam, was placed in donor section of dialysis membrane (effective diffusion area = 2.5 cm^2). Receptor section was filled by an appropriate dissolution medium, such as phosphate buffer (pH 7.4), upheld at 37±0.5 °C and uninterruptedly stirred to ensure sink conditions. At prearranged intermissions, aliquots were withdrawn from receptor compartment and replaced with same volume of fresh medium to preserve constant volume. Withdrawn samples suitably diluted and examined for lornoxicam content by validated UV–visible spectrophotometric method at the drug's characteristic wavelength. Cumulative percentage of drug released got calculated and plotted against time to obtain release profile. The release data were further subjected to kinetic modeling to elucidate mechanism of drug release, including evaluation of diffusion-controlled behavior consistent with Higuchi kinetics.

Preparation of lornoxicam-transethosomal gel

Optimized lornoxicam-transethosomal suspension (LRNX12) incorporated into a Carbopol934 gel base to develop transethosomal gel formulation suitable for transdermal application. Carbopol934 was dispersed in distilled water at several concentrations (0.5, 1.0, and 1.5% w/v) under continuous magnetic stirring to ensure uniform wetting of the polymer. The dispersions were allowed to hydrate and swell overnight at room temperature to achieve complete polymer hydration and optimal gel consistency. Subsequently, triethanolamine was added dropwise under gentle stirring to neutralize the dispersion and induce gel formation, with pH adjusted to near-physiological choice of 6.8 to 7.4 to ensure skin compatibility.

Among the tested concentrations, the 1% w/v Carbopol 934 gel exhibited optimum clarity, smooth texture, appropriate viscosity, and good spread ability, making it suitable for incorporation of the transethosomal suspension. The optimized lornoxicam-loaded transethosomal dispersion (LRNX12) was then slowly incorporated into prepared base with continuous stirring to ensure even distribution of vesicles throughout the gel matrix and to avoid vesicle rupture or aggregation. Stirring was sustained till a homogeneous and smooth transethosomal gel obtained. The final formulation was allowed to equilibrate for 24 hand stored in airtight containers at ambient conditions until more evaluation [20–24].

Evaluation of transethosomal gel

Compatibility studies

Drug–excipient compatibility studies of transethosomal gel formulation were conducted by FTIR spectroscopy. The spectra of lornoxicam and the physical mix of lornoxicam with formulation ingredients corresponding to the optimized gel formulation were recorded and compared. The spectra were analyzed for occurrence, shifting, or disappearance of distinctive absorption peaks of lornoxicam [26].

Physical assessment

The prepared lornoxicam-loaded transethosomal gel was visually inspected for colour, clarity, transparency, and homogeneity. The formulation was examined for the presence of any particulate matter, phase separation, or grittiness to ensure uniformity and acceptable aesthetic properties suitable for topical application [27].

Viscosity

Viscosity of lornoxicam-loaded transethosomal gel was measured by Brookfield DV-I Viscometer (India). Measurement was done at 25±1 °C using an appropriate spindle at a rotational speed of 60 rpm. A sufficient quantity of gel was placed in a beaker to ensure proper immersion of the spindle, and the viscosity values were recorded once a steady reading was obtained [25].

pH measurement

pH of lornoxicam-loaded transethosomal gel was measured by digital pH meter which has been standardized with buffer solutions of pH 4.0 and 7.0. A precisely weighed amount of gel was diluted in 100 ml of distilled water and kept undisturbed for 2h at ambient temperature to allow equilibration. The pH readings were recorded to evaluate formulation's suitability for topical application and skin compatibility [26].

Drug content

For the estimation of drug content, 1 g of the lornoxicam-loaded transethosomal gel was exactly weighed and placed in a 50 ml flask. Methanol got added to solubilize gel base, followed by sonication to facilitate complete extraction of lornoxicam. The obtained solution was then filtered and appropriately diluted with methanol [27, 28]. Absorbance of final solution was recorded at 376 nm by UV–Visible spectrophotometer, employing methanol as blank. The drug content quantified from a previously constructed calibration curve and expressed as a percentage of theoretical content using the corresponding equation:

$$\text{Drug content (\%)} = \frac{\text{Practical content}}{\text{Theoretical drug content}} \text{X } 100$$

Spread ability

Spreadability, an important parameter influencing patient compliance and ease of application, was evaluated using the glass slide method. A fixed glass slide was placed on a horizontal surface, and a known quantity of gel was placed at its center. A second slide was placed over the gel, and a standard weight was applied to facilitate spreading. Time taken for upper slide to move a specified distance recorded, and spread ability got calculated, reflecting ability of the gel to spread uniformly over skin surface [29].

***In vitro* skin permeation study using franz diffusion cell**

In vitro permeation evaluation of lornoxicam-loaded transethosomal gel was carried out using a Franz diffusion apparatus (effective diffusion area = 2.5 cm^2) equipped with a Strat-M® synthetic membrane. A measured quantity of gel (1 g), corresponding to 80 mg of lornoxicam, was placed in donor chamber, whereas phosphate-buffered saline (PBS, pH 7.4) served as receptor medium. Receptor compartment was thermostatically controlled at 37±0.5 °C and kept under constant stirring for the entire duration of the experiment. Samples of 1 ml were taken out from receptor phase at prearranged intermissions over a 24 h period and instantly replaced with same amount of fresh PBS to reserve sink conditions. Cumulative amount of lornoxicam permeated per unit surface area (µg/cm^2) was determined by UV–Visible spectrophotometric analysis at 376 nm. Key permeation parameters like steady-state flux (J), permeability coefficient (Kp), and enhancement ratio (ER), were subsequently calculated to evaluate the transdermal permeation performance and sustained permeation potential of the formulation [30, 31].

Stability studies

A short-term stability study of the optimized lornoxicam-loaded transethosomal gel was conducted for three months at 25±2 °C. Formulation was assessed at 30-day intervals for variations in physical appearance, pH, and drug content to assess its physicochemical stability and suitability for topical use over time [32, 33].

RESULTS AND DISCUSSION

Optimization of lornoxicam-loaded transethosomes

The optimization of lornoxicam-loaded transethosomes was systematically supported by a 3-factor, 3-level BBD to elucidate influence of formulation attributes on critical quality, namely vesicle size (Y_1, PS) and EE (Y_2, %EE). RSM enabled the development of statistically significant quadratic models describing the complex, non-linear relationships between phospholipid (soya lecithin), Tween 80, and ethanol concentrations and the selected responses.

Effect of formulation variables on vesicle size

Model fitting statistics clearly demonstrated that the quadratic model was the most appropriate for describing the response. This was supported by a highly significant sequential p-value (<0.0001) and a non-significant lack-of-fit (p = 0.9035), confirming excellent model adequacy. In contrast, the linear model, despite a statistically significant sequential p-value (0.0056), exhibited a highly significant lack-of-fit (p<0.0001) along with comparatively low adjusted R^2 (0.5181) and predicted R^2 (0.2904), indicating poor explanatory and predictive capability. Similarly, the 2FI model was unsuitable, as reflected by a non-significant sequential p-value (0.8923), significant lack-of-fit (p<0.0001), and a negative predicted R^2 (–0.4392), signifying unreliable prediction performance. The cubic model was aliased and therefore not considered further (table 4 and table 5).

Table 4: Fit summary response 1-particle size

Source	Sequential p-value	Lack of fit p-value	Adjusted R^2	Predicted R^2	Model status
Linear	0.0056	<0.0001	0.5181	0.2904	Not suitable
2FI	0.8923	<0.0001	0.4094	-0.4392	Not suitable
Quadratic	<0.0001	0.9035	0.9984	0.9977	Suggested
Cubic	0.9035		0.9975		Aliased

Table 5: ANOVA results obtained for size of transethosomes

Source	Sum of squares	df	Mean square	F-value	p-value	Remark
Model	8297.39	9	921.93	1098.85	<0.0001	significant
A-Soya lecithin	2492.18	1	2492.18	2970.42	<0.0001	
B-Ethanol	729.62	1	729.62	869.63	<0.0001	
C-Tween 80	1830.13	1	1830.13	2181.32	<0.0001	
AB	51.84	1	51.84	61.79	0.0001	
AC	92.16	1	92.16	109.85	<0.0001	
BC	42.25	1	42.25	50.36	0.0002	

A^2	1980.87	1	1980.87	2360.99	<0.0001	
B^2	841.85	1	841.85	1003.40	<0.0001	
C^2	186.76	1	186.76	222.60	<0.0001	
Residual	5.87	7	0.8390			
Lack of Fit	0.7050	3	0.2350	0.1819	0.9035	not significant
Pure Error	5.17	4	1.29			
Cor total	8303.26	16				

The selected quadratic model exhibited excellent goodness-of-fit, with a very high adjusted R^2 (0.9984) and predicted R^2 (0.9977), indicating that more than 99% of the variability in the response was accurately explained and predicted by the model. The close agreement between adjusted and predicted R^2 values further confirmed the robustness and reliability of the model. ANOVA results revealed that the quadratic model was highly significant ($p<0.0001$), with a large F-value (1098.85), demonstrating strong statistical validity. The lack-of-fit was not significant, confirming that the model adequately fits the experimental data within the studied design space.

All linear terms, soya lecithin (A), ethanol (B), and Tween 80 (C)—exerted a statistically significant influence on the response ($p<0.0001$). Among them, soya lecithin showed the most dominant effect, suggesting that increased lipid concentration strongly governs vesicle size, likely due to enhanced bilayer thickness and vesicle expansion. The interaction terms AB, AC, and BC were also highly significant, highlighting the presence of strong synergistic and antagonistic interactions among formulation variables. Additionally, the significant quadratic terms A^2, B^2, and C^2 confirmed pronounced curvature effects, indicating that the response is governed by nonlinear relationships rather than simple linear trends. Overall, these statistical findings confirm that the quadratic model provides an excellent balance of significance, explanatory power, and predictive accuracy, and was therefore selected as the suggested model for describing the formulation behaviour. Ethanol played a particularly critical role, as reflected by its large quadratic coefficient. Moderate ethanol concentrations reduced vesicle size by enhancing membrane flexibility and promoting vesicle deformation, whereas excessive ethanol increased vesicle size due to bilayer expansion and vesicle fusion. These findings align with the established mechanism of ethanol-induced lipid fluidization reported in transethosomal literature.

The adequacy and robustness of the selected quadratic model were further confirmed through diagnostic and response surface analyses (fig. 1 to fig. 4). The predicted versus actual plot showed excellent agreement between experimental and model-predicted vesicle size values, with data points closely aligned along the 45° reference lines and predicted responses ranging from 136.9 to 210.6 nm, indicating high predictive accuracy. The internally studentized residuals versus predicted values plot exhibited a random scatter within acceptable limits, with no systematic trends or extreme outliers, confirming homoscedasticity and the absence of model bias. Two-dimensional contour analysis revealed distinct elliptical contours, demonstrating significant interaction effects among formulation variables and a clear curvature in the response, with the minimum vesicle size region observed at approximately 149.6 nm within the design space. The three-dimensional response surface plot further illustrated a smooth, well-defined curved surface, reflecting strong quadratic effects and interdependence of variables, consistent with the highly significant model statistics ($F = 1098.85$, $p<0.0001$) and excellent goodness-of-fit parameters (adjusted $R^2 = 0.9984$; predicted $R^2 = 0.9977$). Collectively, these graphical diagnostics and numerical indicators confirm that the quadratic model reliably explains and predicts vesicle size variations across the studied formulation range.

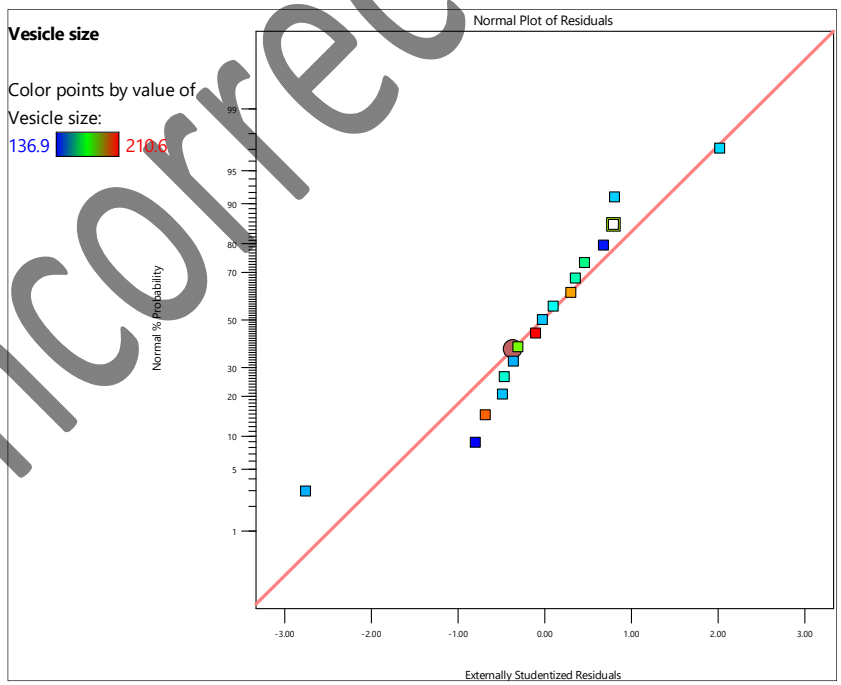

Fig. 1: Predicted versus actual plot for vesicle size

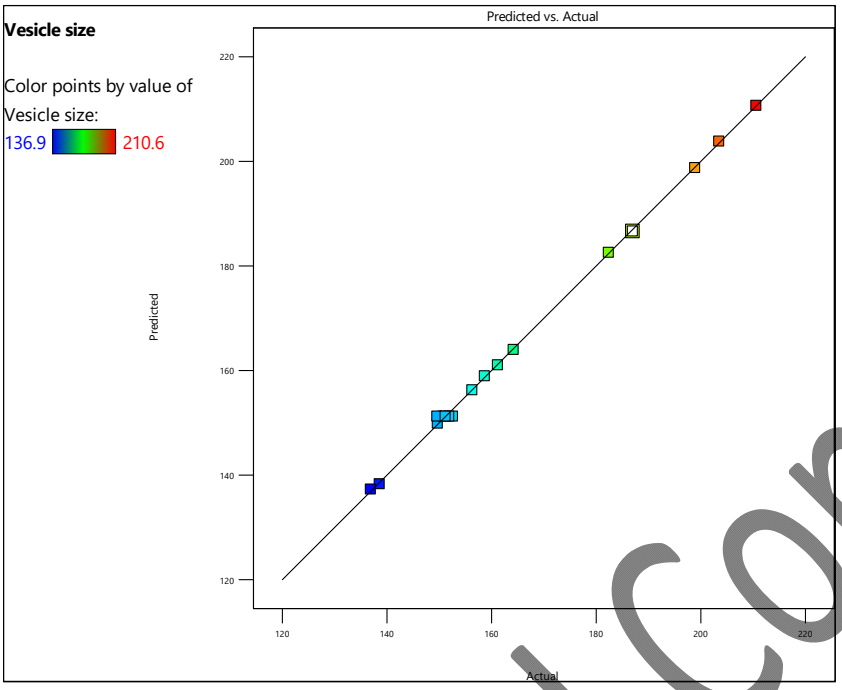

Fig. 2: Internally studentized residuals versus predicted values plot

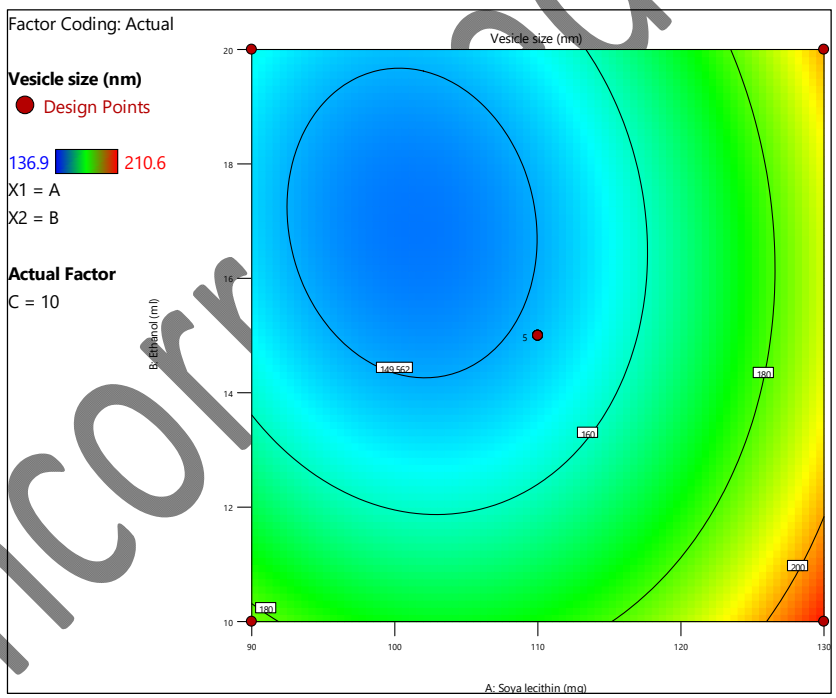

Fig. 3: Two-dimensional contour plot showing the combined effect of formulation variables on vesicle size

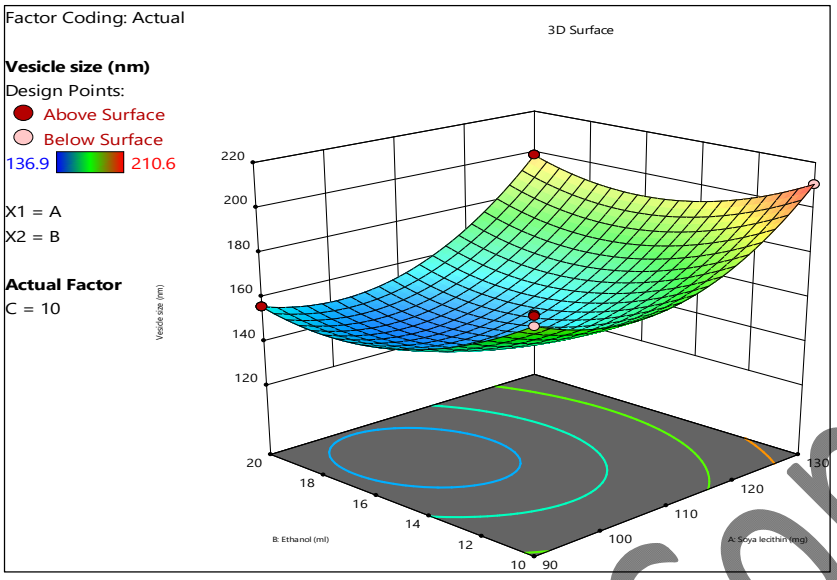

Fig. 4: Three-dimensional response surface plot depicting the effect of formulation variables on vesicle size

Effect of formulation variables on entrapment efficiency

Model comparison statistics confirmed that the quadratic model was the most appropriate for describing the response. The transition from the 2FI to the quadratic model resulted in a highly significant improvement (Quadratic vs 2FI: F = 112.51, p<0.0001), whereas the linear model, despite being significant versus the mean (F = 26.24, p<0.0001), was inadequate due to lack of higher-order effects. The 2FI model showed no significant improvement over the linear model (p = 0.9909), and the cubic model was aliased (p = 0.5925) and therefore not considered further. ANOVA of the selected quadratic model demonstrated that the model was highly significant (F = 272.11, p<0.0001) with a low residual mean square (0.1975), indicating good model precision. Among the linear terms, soya lecithin (A) exhibited the strongest effect (F = 1757.78, p<0.0001), followed by ethanol (B) (F = 209.65, p<0.0001) and Tween 80 (C) (F = 140.51, p<0.0001), confirming their dominant influence on the response. Interaction terms AB, AC, and BC were not statistically significant (p>0.05), suggesting limited interactive effects within the studied range. However, the quadratic terms A^2 (F = 191.87, p<0.0001) and C^2 (F = 117.73, p<0.0001) were highly significant, indicating pronounced curvature effects, while B^2 showed a weaker, non-significant contribution (p = 0.0905). Importantly, the lack-of-fit was not significant (F = 0.7148, p = 0.5925), confirming that the quadratic model adequately fits the experimental data. Overall, these statistical outcomes validate the quadratic model as robust, reliable, and suitable for accurately describing and predicting the response within the design space (table 6 and table 7).

Table 6: Fit summary response 2-entrapment efficiency

Source	Sum of squares	df	mean square	F-value	p-value	Model status
mean vs Total	85172.41	1	85172.41			Not suitable
Linear vs Mean	416.32	3	138.77	26.24	<0.0001	Not suitable
2FI vs Linear	0.7050	3	0.2350	0.0345	0.9909	Not suitable
Quadratic vs 2FI	66.66	3	22.22	112.51	<0.0001	Suggested
Cubic vs Quadratic	0.4825	3	0.1608	0.7148	0.5925	Aliased
Residual	0.9000	4	0.2250			Not suitable
Total	85657.47	17	5038.67			Not suitable

Table 7: ANOVA results obtained for the entrapment efficiency of the transethosomal formulations

Source	Sum of squares	df	Mean square	F-value	p-value	Remark
Model	483.68	9	53.74	272.11	<0.0001	significant
A-Soya lecithin	347.16	1	347.16	1757.78	<0.0001	
B-Ethanol	41.41	1	41.41	209.65	<0.0001	
C-Tween 80	27.75	1	27.75	140.51	<0.0001	
AB	0.1225	1	0.1225	0.6203	0.4568	
AC	0.1600	1	0.1600	0.8101	0.3980	
BC	0.4225	1	0.4225	2.14	0.1870	
A^2	37.89	1	37.89	191.87	<0.0001	
B^2	0.7605	1	0.7605	3.85	0.0905	
C^2	23.25	1	23.25	117.73	<0.0001	
Residual	1.38	7	0.1975			
Lack of Fit	0.4825	3	0.1608	0.7148	0.5925	not significant
Pure Error	0.9000	4	0.2250			
Cor total	485.06	16				

The statistical parameters further confirmed the robustness and reliability of the developed model. The model exhibited a low standard deviation (0.444) relative to the mean response (70.78), resulting in a very low coefficient of variation (0.629%), which indicates excellent precision and high experimental reproducibility. The coefficient of determination (R^2 = 0.9971) demonstrated that more than 99% of the variability in the response was explained by the model. The close agreement between the adjusted R^2 (0.9935) and predicted R^2 (0.9812) values reflects strong model stability and reliable predictive capability. Furthermore, the adequate precision value of 55.34, which is substantially higher than the desirable threshold of 4, indicates an excellent signal-to-noise ratio and confirms that the model can be effectively used to navigate and optimize the design space (table 8).

Table 8: Fit statistics for quadratic model

Statistical parameter	Value
Std. Dev.	0.444
Mean	70.78
C. V. (%)	0.629
R^2	0.9971
Adjusted R^2	0.9935
Predicted R^2	0.9812
Adequate Precision	55.3401

The diagnostic and response surface plots further substantiated the adequacy and predictive reliability of the developed quadratic model for the response. The predicted versus actual plot showed a strong linear correlation, with experimental values closely aligned to the 45° reference line and predicted responses ranging from 59.8 to 78.6, indicating minimal prediction error. The internally studentized residuals plot exhibited random dispersion around zero without any discernible trend or outliers, confirming homoscedasticity and the absence of systematic bias in the model. The two-dimensional contour plot revealed smooth, curved and nearly elliptical contour lines, demonstrating a clear nonlinear relationship between the formulation variables and the response, with an optimum region observed at approximately 76.86, corresponding to the central design point. This trend was further validated by the three-dimensional response surface plot, which displayed a well-defined curved surface with a gradual gradient, highlighting strong quadratic effects and confirming that the response increased progressively within the studied factor levels. The close agreement between experimental and predicted values, together with the narrow response range and smooth surface morphology, is consistent with the excellent model statistics (R^2 = 0.9971, adjusted R^2 = 0.9935, predicted R^2 = 0.9812) and high signal-to-noise ratio (adequate precision = 55.34), collectively confirming that the model is robust, precise, and suitable for navigating the design space and identifying optimal formulation conditions (fig. 5 to fig. 8).

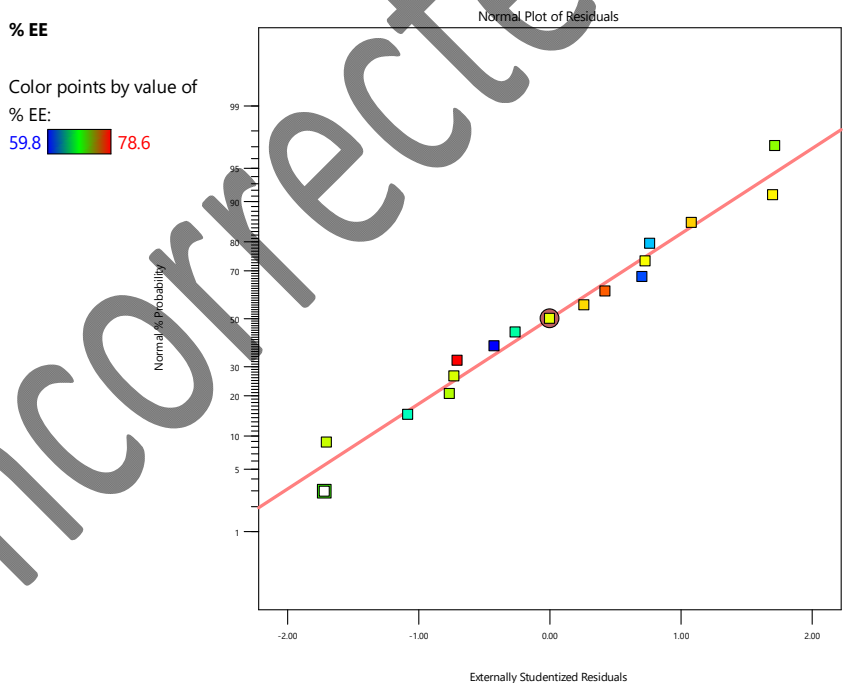

Fig. 5: Predicted versus actual plot illustrating the agreement between experimental and model-predicted response values

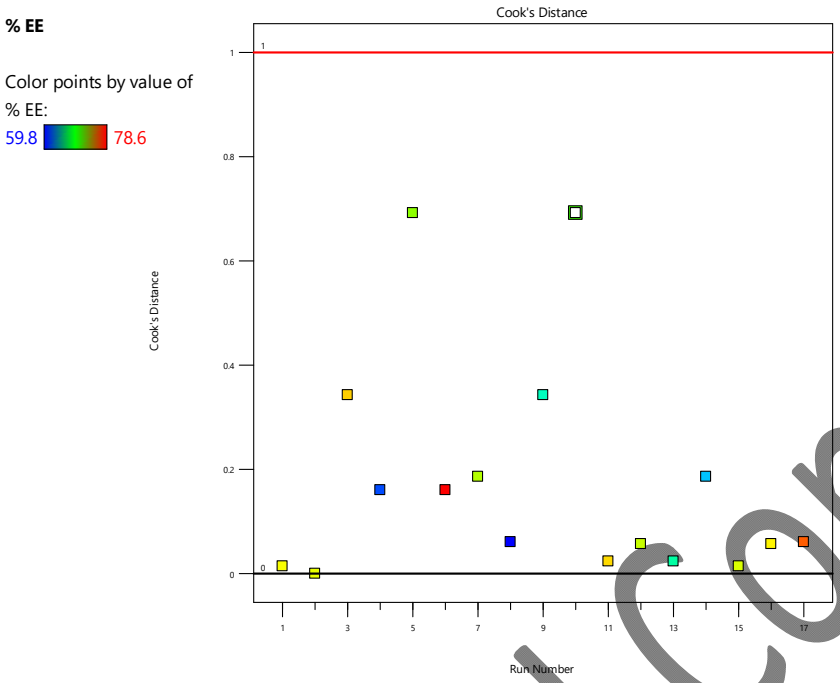

Fig. 6: Plot of internally studentized residuals versus predicted response values for model diagnostic evaluation

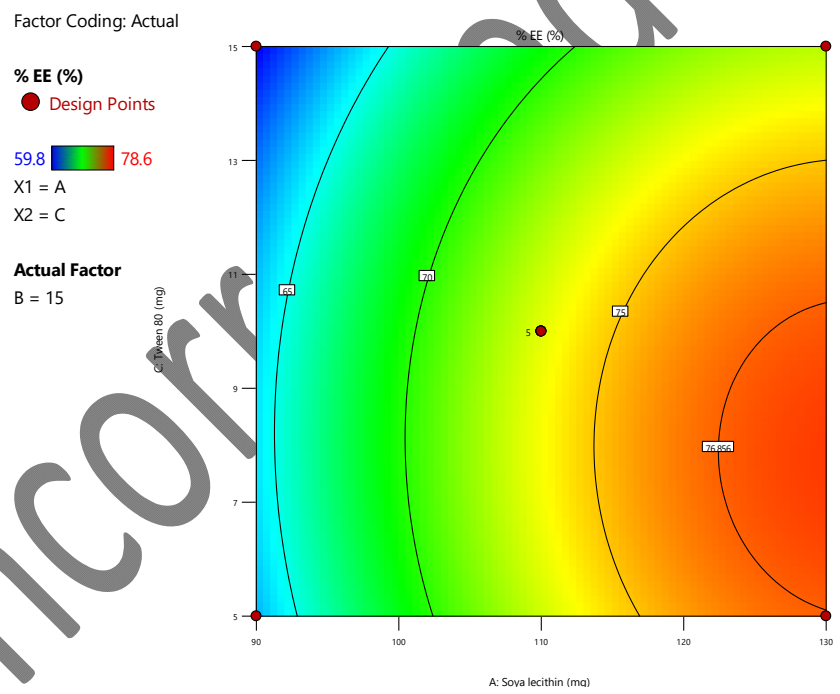

Fig. 7: Two-dimensional contour plot showing the combined effect of formulation variables on the response

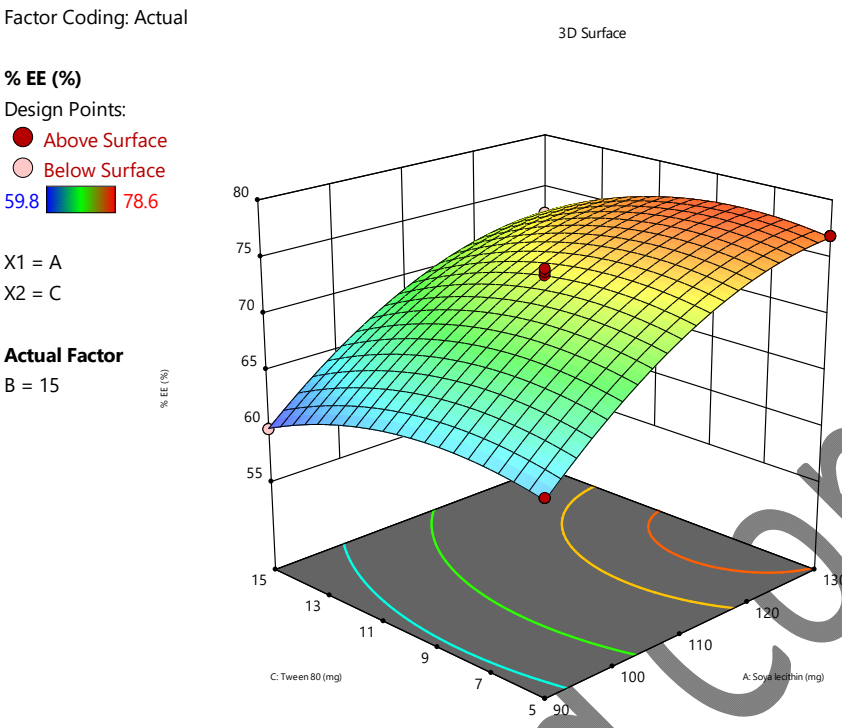

Fig. 8: Three-dimensional response surface plot depicting the influence of formulation variables on the response

Significant quadratic terms (A^2, B^2, and C^2) indicated curvature effects, confirming that EE does not increase linearly beyond optimal concentrations. This phenomenon is consistent with previously reported transethosomal systems, where excessive ethanol or surfactant leads to membrane thinning and drug leakage. Interaction analysis demonstrated a significant AB interaction (lecithin–Tween 80), highlighting the synergistic balance between lipid rigidity and surfactant-induced elasticity required for optimal drug entrapment.

The polynomial equation generated for %EE confirmed that both synergistic and antagonistic effects govern drug entrapment behavior, emphasizing the necessity of multivariate optimization rather than single-factor experimentation.

Optimization and selection of final formulation

Optimization via desirability function

The optimized formulation corresponded to 1.13% w/v soya lecithin, 0.13% v/v Tween 80, and 17.8% v/v ethanol, yielding nanosized vesicles with high EE and overall desirability of 0.824. Close agreement among predicted and experimental values confirmed accuracy of optimization model. LRNX12 formulation closely matched these optimized conditions and was therefore selected for further characterization.

Compatibility of transethosomal formulation

Pure lornoxicam exhibited its distinctive absorption bands corresponding to N–H stretching in region of 3300–3400 cm^{-1}, C=O stretching around 1650–1700 cm^{-1}, and characteristic aromatic and sulfonyl vibrations in the fingerprint region (1500–700 cm^{-1}), confirming the chemical integrity of the drug. The excipients (soya lecithin, Tween 80, and ethanol) showed their typical broad O–H stretching bands, aliphatic C–H stretching, and ester or ether-related vibrations at expected wave numbers. In the physical mixture, all major characteristic peaks of lornoxicam and the excipients were retained without any significant shift, disappearance, or emergence of new peaks, indicating the absence of chemical interaction and confirming simple physical blending. Similarly, the FTIR spectrum of lornoxicam-loaded transethosomes preserved the principal characteristic peaks of lornoxicam at their original positions, with only minor changes in peak intensity attributable to entrapment and dilution effects. The lack of peak shifting or new band formation demonstrates good compatibility between lornoxicam and the formulation components and confirms that the drug remains chemically stable within the transethosomal system. The FTIR spectra illustrates the characteristic functional group vibrations of pure lornoxicam, soya lecithin, Tween 80, ethanol, their physical mixture, and the lornoxicam-loaded transethosomal formulation (fig. 9).

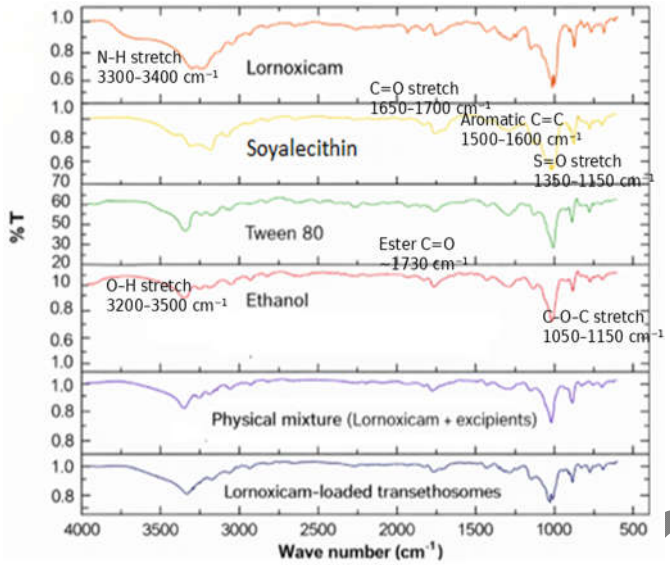

Fig. 9: FTIR spectra of lornoxicam, formulation excipients, physical mixture, and lornoxicam-loaded transethosomes

Particle size determination

The transethosomal formulation showed a narrow and well-defined size distribution within the nanometer range, confirming effective size reduction and vesicle formation. The marked decrease in particle size following transethosomal entrapment enhances surface area, improves physical stability, and supports better drug dispersion, which is advantageous for transdermal delivery and overall formulation performance. The particle size distribution analysis demonstrates a clear difference between pure lornoxicam and the lornoxicam-loaded transethosomal formulation (fig. 10).

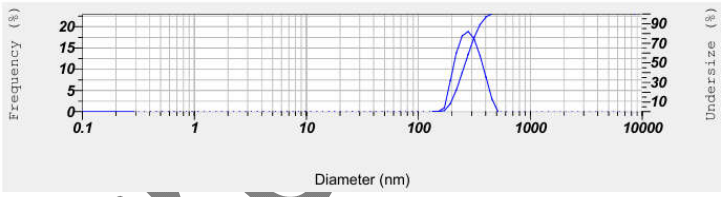

(B)

Fig. 10: Particle size distribution profile of pure lornoxicam (A), lornoxicam-loaded transethosomal formulation (B)

Polydispersity index

The lornoxicam-loaded transethosomal formulations showed markedly lower PDI values ranging from 0.21 to 0.34, reflecting a narrow and homogeneous vesicle size distribution. The optimized formulation (LRNX12) demonstrated a PDI of approximately 0.24, confirming excellent uniformity and dispersion stability. These lower PDI values indicate reduced polydispersity, enhanced formulation reproducibility, and improved physical stability, which are critical attributes for efficient and consistent transdermal drug delivery systems.

Zeta potential

The zeta potential analysis demonstrated a marked difference between pure lornoxicam and the lornoxicam-loaded transethosomal formulation. Pure lornoxicam exhibited a zeta potential of −21 mV, indicating relatively low electrostatic stabilization and a greater tendency for particle aggregation. In contrast, the lornoxicam-loaded transethosomes showed a significantly higher negative zeta potential of −34.6mV, reflecting enhanced surface charge and improved electrostatic repulsion between vesicles. The negative zeta potential (−34.6 mV) arises from ionized phosphate head groups of soya lecithin and ethanol-induced surface charge redistribution, conferring strong electrostatic repulsion and enhanced colloidal stability. The increase in negative zeta potential upon transethosomal entrapment suggests superior colloidal stability of the formulation, which can be credited to combined impacts of phospholipids, ethanol, and edge activators. These results confirm that incorporation of lornoxicam into transethosomes substantially improves its physicochemical stability, supporting the suitability of the formulation for further development (fig. 11).

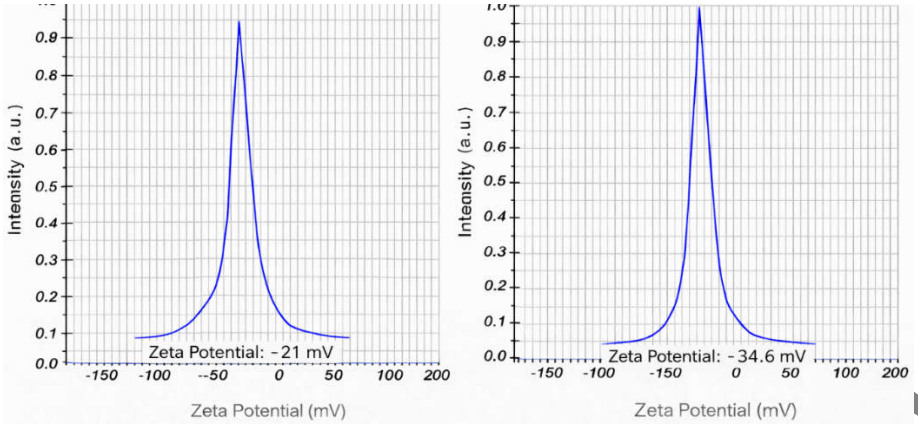

(a) **(b)**

Fig. 11: Zeta potential distribution profiles of (a) pure lornoxicam and (b) lornoxicam-loaded transethosomal formulation

DSC thermograms

DSC thermogram of lornoxicam showed a sharp endothermic peak indicating its melting point, confirming its crystalline properties. Soya lecithin, Tween 80, and ethanol exhibited broad or weak thermal transitions characteristic of amorphous polymers and liquid components, mainly associated with moisture loss or thermal relaxation rather than true melting. In the physical mixture, the characteristic melting endotherm of lornoxicam was retained at a similar temperature without any significant shift, indicating the absence of drug–excipient incompatibility. In contrast, the lornoxicam-loaded transethosomes displayed a marked reduction or suppression of the drug's melting peak, signifying effective entrapment of lornoxicam within transethosomal matrix and partial conversion of the drug to an amorphous or molecularly dispersed state. These findings confirm good thermal compatibility of lornoxicam with the formulation components and support effective drug incorporation into the transethosomal system (fig. 12). Although DSC suggests partial amorphization of lornoxicam, definitive confirmation of crystallinity changes requires XRPD analysis, which is recommended for future studies.

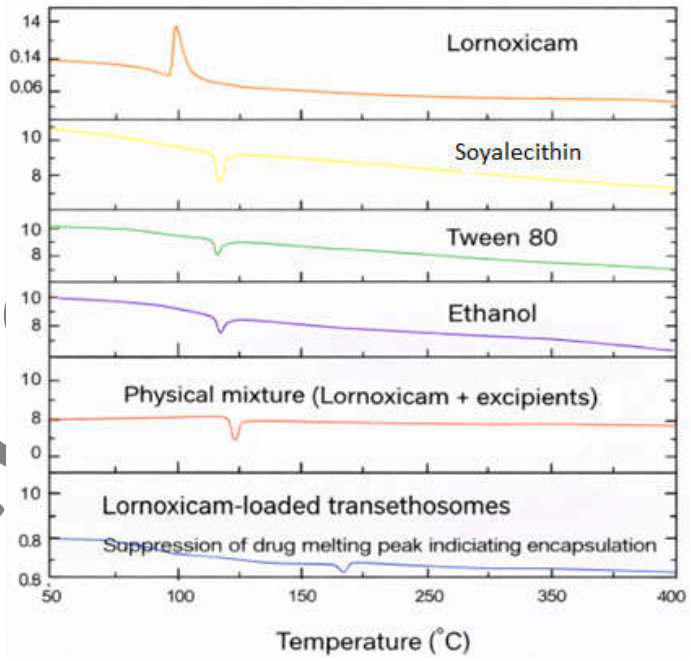

Fig. 12: DSC thermograms of lornoxicam, soya lecithin, Tween 80, ethanol, physical mixture of lornoxicam with excipients, and lornoxicam-loaded transethosomes

Transmission electron microscopy

Temi mages reveal morphological characteristics of optimized formulation at different magnifications. At the 200 nm scale, the particles appear predominantly discrete with near-spherical to slightly irregular shapes, indicating successful formation of nanosized entities with relatively uniform distribution, although mild aggregation is visible, which is common for lipid-or polymer-based nano systems during sample drying (fig. 13). The observed contrast variations in TEM images indicate heterogeneity in electron density, which may be attributed to lipid bilayer organization and vesicle thickness. However, definitive localization of the drug cannot be confirmed without elemental mapping, and therefore interpretations are limited to morphological observations. At the lower magnification (500 nm scale), clusters of nanoparticles are observed, suggesting secondary

aggregation; however, individual particles remain within the nanometric range, supporting the particle size data obtained from dynamic light scattering (fig. 14). Overall, the TEM observations corroborate the nanoscale size, morphology, and structural integrity of the formulation, validating the suitability of the developed system for further pharmaceutical application (fig. 13 and fig. 14).

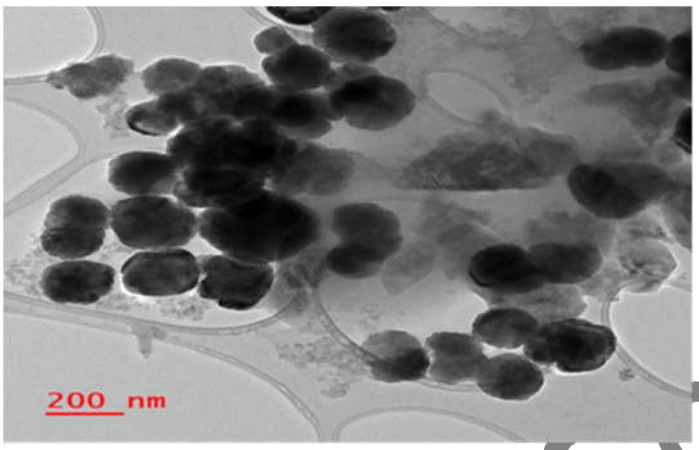

Fig. 13: TEM images of optimized formulation showing nanosized particles with near-spherical morphology at 200 nm scale

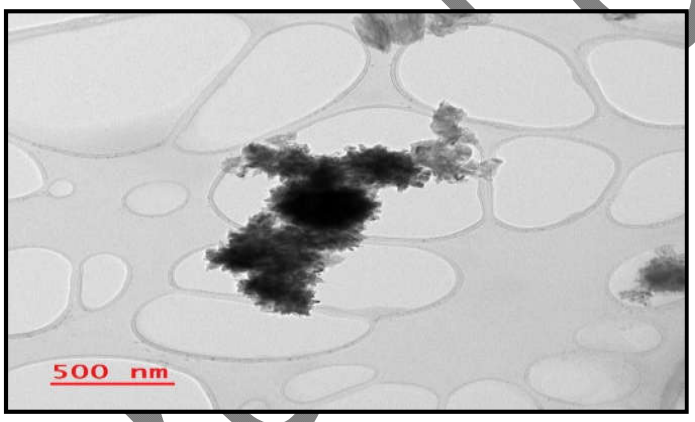

Fig. 14: TEM images of optimized formulation showing nanosized particles with near-spherical morphology at 500 nm scale

The optical microscopy image shows the formation of well-defined, spherical droplets with a uniform distribution, indicating successful emulsification and good droplet stability of the formulation suitable for entrapment. The presence of discrete, circular droplets with smooth boundaries suggests effective reduction of interfacial tension by the formulation components, while the absence of extensive coalescence or irregular structures reflects adequate stabilization of the dispersed phase. The variation in droplet size observed across the field is typical of emulsified systems prior to further size reduction steps and supports the suitability of the formulation composition for nanoscale processing (fig. 15).

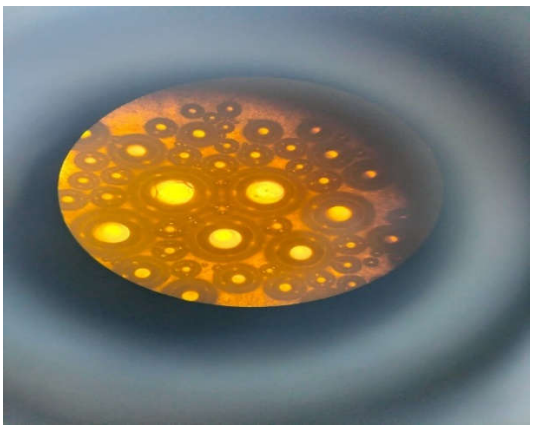

Fig. 15: Optical microscopy image of the formulated system showing spherical, uniformly distributed emulsion droplets, indicating effective emulsification and structural stability of the formulation (10X magnification)

Entrapment efficiency

The %EE of lornoxicam in the transethosomal formulations (LRNX1–LRNX14) ranged from approximately 58.4% to 81.8%, indicating effective drug incorporation across the formulation batches. Among these, the optimized formulation LRNX12 exhibited the highest EE of about 81.8%, demonstrating a clear improvement compared with other formulations. The high EE can be attributed to the optimized phospholipid–ethanol ratio and the fluidizing effect of ethanol, which enhanced drug solubilization and accommodation within the vesicular bilayer. In contrast, formulations with lower lipid content or suboptimal ethanol levels showed comparatively reduced entrapment, likely due to insufficient bilayer capacity to retain the drug. Overall, the high EE achieved with LRNX12 highlights the advantage of the transethosomal system in maximizing drug loading, minimizing drug loss, and supporting sustained transdermal delivery of lornoxicam.

***In vitro* drug release from transethosomes**

Lornoxicam-loaded transethosomal formulation (LRNX12) exhibited a characteristic biphasic release profile, consisting of an early eruption by sustained drug release over 24 h. Approximately 22% of lornoxicam was released within first hour, which can be accredited to drug molecules loosely associated with the vesicle surface or present in the outer lipid bilayer. This initial release is advantageous for rapid onset of anti-inflammatory action. Subsequently, a controlled and prolonged release phase was observed, reaching 94.7% cumulative release at 24 h (table 9, fig. 16). The release data were fitted to zero-order, first-order, Higuchi, and Korsmeyer–Peppas models. The highest correlation coefficient was obtained for the Higuchi model (R^2 = 0.97), indicating diffusion-controlled release. An n value of approximately 0.48 obtained from the Korsmeyer–Peppas model indicates a Fickian diffusion–controlled release mechanism, wherein drug transport is primarily driven by concentration gradients. This diffusion-dominant behavior is attributed to the organized vesicular structure, with lornoxicam either entrapped within the aqueous core or associated with the lipid bilayer, allowing controlled diffusion across the vesicle membrane. The absence of anomalous or erosion-controlled release further supports the structural integrity and stability of the vesicular system during the release period.

Table 9: Percentage drug release of the lornoxicam-loaded transethosomal formulation (LRNX12)

Time (h)	Cumulative % drug release of lornoxicam-loaded transethosomes
0	0.00± 0.00
1	22.8± 0.05
2	34.6± 0.26
4	48.9± 0.34
6	53.1± 1.28
8	59.5± 0.22
10	64.5± 0.11
12	73.1± 0.39
14	77.0± 1.14
16	82.2± 0.21
18	84.4± 1.22
20	86.9± 0.18
21	89.7± 0.19
22	91.3± 1.08
24	94.7± 0.42

All values are articulated as mean±SD (n = 3)

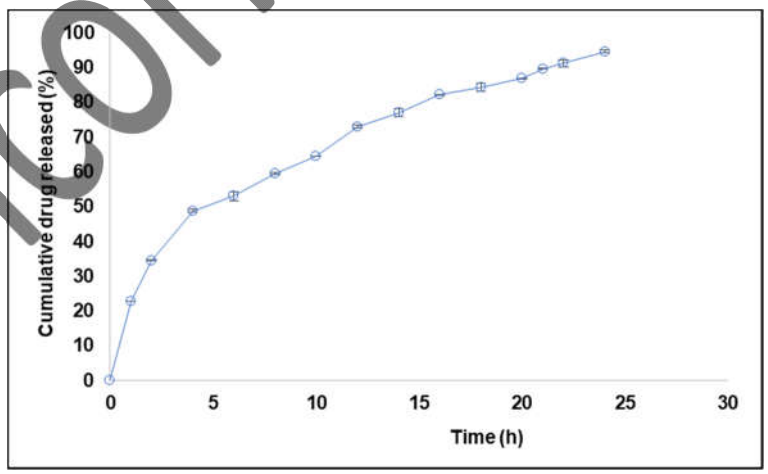

Fig.16: Cumulative % drug release of the lornoxicam-loaded transethosomal formulation (LRNX12), All values are articulated as mean±SD (n = 3)

Evaluation of transethosomal gel parameters

Transethosomal gel compatibility

The FTIR spectra showed the characteristic functional group vibrations of pure lornoxicam, Carbopol 934, the physical mixture, lornoxicam-loaded transethosomes, and the transethosomal gel formulation. Pure lornoxicam displayed its typical N–H stretching (3300–3400 cm^{-1}), amide C=O stretching (1650–1700 cm^{-1}), and aromatic/sulfonyl vibrations in the fingerprint region, confirming its structural integrity, while Carbopol 934 exhibited broad O–H stretching and characteristic carboxylic acid and C–O vibrations. In physical mixture, all distinguishing peaks of lornoxicam and Carbopol 934 were retained without any significant shift or new peak formation. Similarly, both the lornoxicam-loaded transethosomes and the transethosomal gel formulation preserved the major drug peaks at their original positions, with only minor intensity variations due to entrapment and polymeric matrix effects. These findings indicate absence of chemical interaction and confirm good compatibility and chemical stability of lornoxicam within transethosomal and gel formulations (fig. 17).

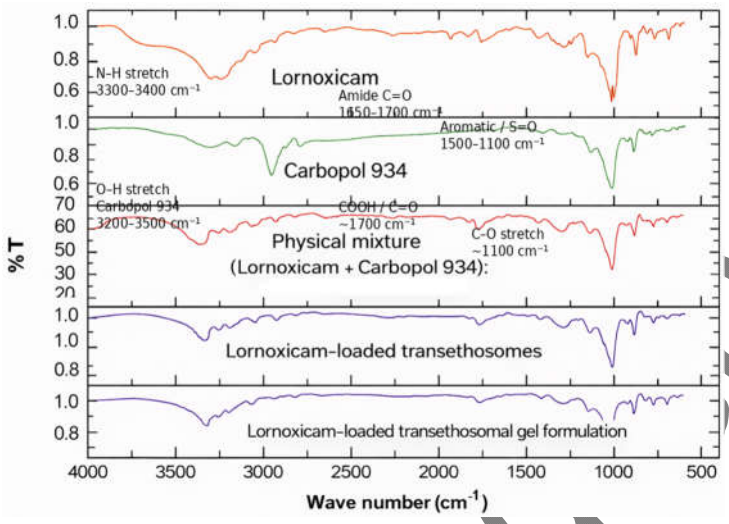

Fig. 17: FTIR spectra of lornoxicam, Carbopol 934, physical mixture, lornoxicam-loaded transethosomes, and lornoxicam-loaded transethosomal gel formulation

Physical parameters

The lornoxicam-loaded transethosomal gel exhibited a uniform colour with a clear to slightly translucent appearance. The formulation was free from visible particulate matter, grittiness, or phase separation, indicating good clarity and stability. Overall, the gel showed excellent homogeneity and smooth texture, confirming acceptable aesthetic properties for topical application.

Viscosity, pH measurement, spreadability, and drug content

The optimized lornoxicam-loaded transethosomal gel (LRNX12) exhibited physicochemical properties appropriate for transdermal application, as summarized in table 10. pH of formulation was 6.2±0.05, which lies within acceptable physiological choice of the skin, indicating minimal risk of irritation upon topical application. Maintaining a near-skin pH is particularly important for long-term use, as deviations may compromise skin integrity and patient compliance. The drug content analysis of the lornoxicam-loaded transethosomal gel revealed uniform drug distribution, with the drug content found to be 98.4±1.2%, indicating good content uniformity and minimal drug loss during formulation (table 10).

Table 10: Transethosomal gel parameters

Parameter	Result
pH-Measurement	6.2±0.05
Viscosity	5210±25.8 cP
Drug Content	98.4±1.2%
Spreadability	10.82±0.3 g. cm/s

All values are articulated as mean±SD (n = 3)

Viscosity of gel got recorded as 5210±25.8 cP, suggesting an optimal balance between ease of application and sufficient consistency to ensure prolonged residence time at site of applying (table 10). Adequate viscosity prevents rapid runoff from the skin surface while allowing smooth spreading under minimal shear stress. The spreadability value of 10.82±0.3 g·cm/s further confirms good rheological behavior, indicating that the gel can be evenly distributed over the skin with minimal applied force. Collectively, these gel parameters demonstrate that incorporation of transethosomes into Carbopol matrix did not adversely affect the mechanical or aesthetic properties of the formulation and resulted in a patient-friendly dosage form.

***In vitro* skin permeation study using franz diffusion cell**

The *in vitro* skin permeation profile showed a markedly enhanced and sustained permeation of lornoxicam from transethosome-loaded gel compared with the plain gel over a 24 h period. The transethosomal formulation exhibited an initial controlled permeation, reaching 19.2% within 1 h, followed by a gradual and continuous increase in drug permeation, achieving 58.4% at 12 h and a maximum of 93.3% at 24 h. In contrast, the plain gel showed significantly lower permeation at all time points, with only 29.2% permeation at 12 h and 45.0% at 24 h (table 11; fig. 18). The substantially higher permeation from the transethosomal gel can be attributed to the nanosized vesicular structure, enhanced drug solubilization,

and improved diffusion through the gel matrix, confirming the superiority of the transethosome-based system for prolonged and efficient lornoxicam permeation.

Table 11: Drug permeation profiles of transethosomal gel versus plain gel

Time (h)	Cumulative drug permeated (%) from lornoxicam-loaded transethosomal gel	Drug permeated from plain gel
0	0.00± 0.0	0.00±0.0
1	19.2±0.13	8.2±0.13
2	21.5± 0.27	9.8±0.29
4	24.5± 0.43	13.3±0.29
6	35.4± 0.28	15.8±0.25
8	42.7± 1.58	18.2±0.36
10	49.2± 0.59	25.4±1.29
12	58.4± 0.85	29.2±0.42
14	61.8± 0.75	30.5±0.35
16	65.4± 0.13	32.0±0.72
18	67.4± 0.27	36.0±0.71
20	70.3± 0.99	38.0±0.64
22	74.6± 0.71	40.8±0.42
24	93.3± 1.13	45.0±0.71

All values are articulated as mean±SD (n = 3)

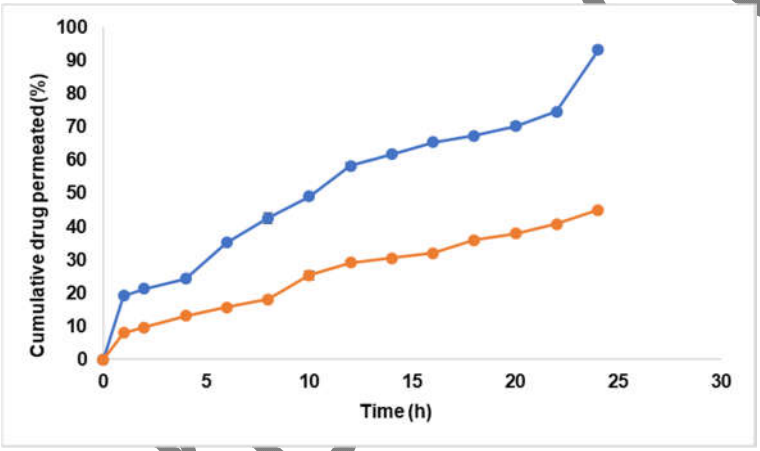

Fig. 18: Cumulative drug permeated (%) profile (blue: drug loaded formulation; orange: plain gel), All readings are articulated as mean (n = 3)

At early points, transethosomal gel showed pointedly higher drug permeation associated to the plain gel, indicating faster onset of drug transport. This behavior can be accredited to combined impacts of ethanol-induced lipid fluidization and ultradeformable nature of transethosomes, which facilitates penetration through intercellular pathways. As time progressed, the permeation from the transethosomal gel continued in a sustained manner, reflecting the reservoir effect of vesicles within the gel matrix and controlled release of lornoxicam. In contrast, the limited permeation observed with the plain gel is likely due to poor aqueous solubility and low diffusivity of free lornoxicam across membrane. These confirm that transethosomal incorporation significantly improves transdermal flux and supports prolonged drug availability, which is desirable for chronic inflammatory conditions.

Stability studies

Stability evaluation of the optimized formulation (LRNX12) over 3 mo at 25±2 °C demonstrated minimal changes in EEand drug content, as presented in table 12. Entrapment efficiency decreased marginally from 87.3% to 83.65%, while drug content showed only a slight reduction from 92.05% to 91.28%. These minor variations are within acceptable limits and indicate good physicochemical stability of the formulation.

Table 12: Effect of stability on entrapment efficiency and drug content

Days	% Entrapment efficiency		%Drug content	
	Before (25±2 °C)	After (25±2 °C)	Before (25±2 °C)	After (25±2 °C)
3 mo	87.3±5.57	83.65±4.34	92.05±7.21	91.28±7.32

All values are articulated as mean±SD (n = 3)

The observed stability can be attributed to the negative zeta potential of the transethosomal vesicles, which provides electrostatic repulsion and avoids vesicle aggregation, as well as protective environment of the gel matrix that minimizes drug leakage and degradation. The stability data suggest that the lornoxicam-loaded transethosomal gel is capable of maintaining its structural integrity and drug-loading capacity during storage,

supporting its potential for practical pharmaceutical application. Overall, the optimized formulation demonstrated favorable gel characteristics, enhanced permeation performance, and satisfactory stability, confirmatory its suitability as an effective transdermal delivery system for lornoxicam.

The stability evaluation performed in the present study represents a short-term preliminary stability assessment conducted at 25±2 ℃ over a period of three months to assess physical appearance, drug content, and entrapment efficiency. While the results indicate acceptable short-term stability under ambient conditions, comprehensive stability profiling in accordance with ICH guidelines, including accelerated stability testing at 40±2 ℃/75±5% RH, is required to establish long-term stability and shelf-life. Such accelerated stability studies are planned as mandatory future work to support regulatory translation and product development.

The observed formulation outcomes can be mechanistically explained by the synergistic interplay between phospholipid concentration, ethanol content, and edge activator presence in the transethosomal system [27]. The significant increase in entrapment efficiency with rising soya lecithin concentration is attributable to enhanced bilayer availability and increased hydrophobic domains capable of accommodating the lipophilic lornoxicam molecule. Similar trends have been reported in previously optimized transethosomal and nanoethosomal systems, where higher phospholipid content resulted in improved drug loading due to increased vesicular volume and bilayer thickness [28]. However, the presence of statistically significant quadratic terms indicates that beyond an optimal concentration, further increases may compromise vesicle integrity, leading to drug leakage and reduced EE.

Ethanol played a critical dual role by improving drug solubilization and increasing bilayer fluidity, thereby facilitating vesicle deformability and transdermal penetration. Moderate ethanol concentrations resulted in reduced vesicle size due to enhanced membrane flexibility, while excessive ethanol caused bilayer expansion and vesicle fusion, leading to size enlargement [29]. This non-linear behavior is consistent with previously reported transethosomal systems, where ethanol-mediated lipid fluidization enhances skin permeation but requires careful optimization to avoid structural destabilization.

The markedly enhanced *in vitro* permeation observed with the transethosomal gel compared with the plain gel can be attributed to multiple complementary mechanisms. Ethanol disrupts the ordered lipid structure of the stratum corneum, increasing its permeability, while the ultradeformable nature of transethosomes enables passage through narrow intercellular pathways. Additionally, incorporation of transethosomes into a Carbopol gel matrix provides a reservoir effect, ensuring prolonged skin contact and sustained drug release [30]. Compared with previously reported lornoxicam ethosomal, niosomal, and conventional topical formulations, the present transethosomal gel demonstrated superior cumulative permeation at 24 h, highlighting the advantage of ethanol–edge activator synergy in achieving enhanced and sustained transdermal delivery.

When compared with other reported vesicular systems for lornoxicam delivery, the optimized transethosomal gel (LRNX-12) demonstrated competitive or superior performance in key formulation parameters. Lornoxicam-loaded niosomal gels have been reported with particle sizes up to ~1.125 µm, entrapment efficiency of ~52.4%, and enhanced permeation of ~31.4 µg/cm^2 versus ~7.37 µg/cm^2 for plain gel over 24 h, indicating approximately 4-fold improvement in skin permeation for the niosomal system relative to plain gel controls[34]. Transfersomal lornoxicam formulations have demonstrated vesicle sizes around 233.5±12.5 nm and very high entrapment efficiency (~99.3%), along with improved permeation and physical stability compared with non-transfersomal hydrogels [35]. Ethosomal systems reported for lornoxicam have achieved ~74.2% cumulative drug permeation at 24 h, reflecting enhanced skin penetration attributable to high ethanol content in the vesicles [36]. In contrast, the optimized transethosomal gel in this study produced nanosized vesicles with high entrapment efficiency and an approximately 2-fold increase in cumulative skin permeation compared with conventional gel, combining the permeation-enhancing effects of ethanol and vesicle deformability. These comparative results collectively demonstrate that the transethosomal system integrates advantages seen in ethosomal and transfersomal platforms, offering a balanced profile of size, entrapment, and permeation for effective lornoxicam transdermal delivery.

Overall, these findings confirm that the optimized transethosomal gel not only improves drug loading and vesicle stability but also significantly enhances transdermal flux and release control. The formulation therefore represents a rational and effective approach for improving the therapeutic performance of lornoxicam while potentially reducing dosing frequency and systemic adverse effects associated with oral administration.

CONCLUSION

Lornoxicam-loaded transethosomal gel demonstrated markedly enhanced transdermal drug delivery, characterized by improved skin permeation, sustained drug release, and promising potential for effective anti-inflammatory therapy. Optimization using a BBD revealed that vesicle size and EE were predominantly governed by phospholipid (soya lecithin) and surfactant (Tween 80) concentrations, while ethanol played a perilous role in modulating membrane fluidity and enhancing permeation. Optimized formulation (LRNX-12) yielded nanosized, physically stable vesicles with a favourable negative zeta potential, and morphological evaluation by TEM confirmed uniformly spherical vesicles with smooth surfaces and minimal aggregation. *In vitro* release indicated a diffusion-controlled release mechanism from vesicular matrix. Moreover, *in vitro* permeation studies demonstrated significantly superior transdermal flux of the transethosomal gel compared with the conventional plain gel, validating its effectiveness in enhancing skin penetration and sustaining lornoxicam delivery. Quantitatively, the optimized transethosomal gel exhibited an approximately 2-fold increase in cumulative drug permeation compared with the plain gel, along with sustained drug release over a 24 h period, indicating prolonged drug availability at the site of action. Short-term stability evaluation over three months at 25±2 ℃ confirmed acceptable physical stability, drug content retention, and entrapment efficiency, supporting formulation robustness under ambient storage conditions. The optimized transethosomal gel achieved 2-fold higher cumulative permeation compared with plain gel and sustained release over 24 h, supporting its suitability for once-daily transdermal therapy. These quantitative improvements justify further pre-clinical evaluation.

ACKNOWLEDGMENT OF AI-GENERATED CONTENT

I acknowledge that generative artificial intelligence (AI) tools were used to assist in language refinement.

FUNDING

Nil

AUTHORS CONTRIBUTIONS

The authors conducted the study, carried out the experiments, and wrote their research plan, review, and revisions. All authors concur in the submission and publishing. All authors have reviewed and consented to the final version of the text for publication.

CONFLICTS OF INTERESTS

The authors declare that they have no competing interests

REFERENCES

1. Radhofer-Welte S, Rabasseda X. Lornoxicam, a new potent NSAID with an improved tolerability profile. Drugs Today (Barc). 2000 Jan;36(1):55-76. doi: 10.1358/dot.2000.36.1.566627, PMID 12879104.
2. Berg J, Fellier H, Christoph T, Grarup J, Stimmeder D. The analgesic NSAID lornoxicam inhibits cyclooxygenase (COX)-1/−2, inducible nitric oxide synthase (iNOS), and the formation of interleukin (IL)-6 *in vitro*. Inflamm Res. 1999 Jul;48(7):369-79. doi: 10.1007/s000110050474, PMID 10450786.
3. Helmy HS, El-Sahar AE, Sayed RH, Shamma RN, Salama AH, Elbaz EM. Therapeutic effects of lornoxicam-loaded nanomicellar formula in experimental models of rheumatoid arthritis. Int J Nanomedicine. 2017 Sep;12:7015-23. doi: 10.2147/IJN.S147738. PMID 29026298.
4. Zhang Y, Zhong D, Si D, Guo Y, Chen X, Zhou H. Lornoxicam pharmacokinetics in relation to cytochrome P450 2C9 genotype. Br J Clin Pharmacol. 2005 Jan;59(1):14-7. doi: 10.1111/j.1365-2125.2005.02223.x. PMID 15606435.
5. Palanati M, Bhikshapathi DV. Development, characterization and evaluation of entrectinib nanosponges loaded tablets for oral delivery. Int J App Pharm. 2023;15(6):269-81. doi: 10.22159/IJAP.2023v15i6.49022.
6. Sohail R, Mathew M, Patel KK, Reddy SA, Haider Z, Naria M et al. Effects of non-steroidal anti-inflammatory drugs (NSAIDs) and gastroprotective NSAIDs on the gastrointestinal tract: A narrative review. Cureus. 2023 Apr;15(4):e37080. doi: 10.7759/cureus.37080, PMID 37153279.
7. Ngcobo NN. Influence of ageing on the pharmacodynamics and pharmacokinetics of chronically administered medicines in geriatric patients: a review. Clin Pharmacokinet. 2025 Mar;64(3):335-67. doi: 10.1007/s40262-024-01466-0, PMID 39798015.
8. Wong WF, Ang KP, Sethi G, Looi CY. Recent advancement of medical patch for transdermal drug delivery. Medicina (Kaunas). 2023 Apr;59(4):778. doi: 10.3390/medicina59040778, PMID 37109736.
9. Porwal P, Shah N, Singh Rao A, Jain I, Maniangat Luke A, Shetty KP et al. Comparative evaluation of efficacy of ketoprofen and diclofenac transdermal patches with oral diclofenac tablet on postoperative endodontic pain- A randomized clinical trial. Patient Prefer Adherence. 2023;17:2385-93. doi: 10.2147/PPA.S421371, PMID 37790865.
10. Haque T, Talukder MM. Chemical enhancer: A simplistic way to modulate barrier function of the stratum corneum. Adv Pharm Bull. 2018 Jun;8(2):169-79. doi: 10.15171/apb.2018.021.
11. Zhao L, Chen J, Bai B, Song G, Zhang J, Yu H et al. Topical drug delivery strategies for enhancing drug effectiveness by skin barriers, drug delivery systems and individualized dosing. Front Pharmacol. 2024 Jan;14:1333986. doi: 10.3389/fphar.2023.1333986, PMID 38293666.
12. Chary SS, Bhikshapathi DV, Vamsi NM, Kumar JP. Optimizing entrectinib nanosuspension: quality by Design for enhanced oral bioavailability and minimized fast-fed variability. BioNanoScience. 2024 Feb;14(4):4551-69. doi: 10.1007/s12668-024-01462-5.
13. Samineni R, Choudhary RK, Sujala DP, Khan A, Gouru SA, Ravindra Babu M et al. A prospective review on novel strategies for preparation and evaluation of nanosponge tablets. Eur Chem Bull. 2023May;12(5):2428-96. doi: not available.
14. Almuqbil RM, Aldhubiab B. Ethosome-based transdermal drug delivery: its structural components, preparation techniques, and therapeutic applications across metabolic, chronic, and oncological conditions. Pharmaceutics. 2025 Apr;17(5):583. doi: 10.3390/pharmaceutics17050583.
15. Abdallah MH, Shahien MM, El-Horany HE, Ahmed EH. Modified phospholipid Vesicular Gel for transdermal Drug Delivery: the Influence of glycerin and/or ethanol on Their Lipid Bilayer Fluidity and Penetration Characteristics. Gels. 2025 May;11(5):358. doi: 10.3390/gels11050358, PMID 40422378.
16. Malang SD, Shambhavi SAN, Sahu AN. Transethosomal gel for enhancing transdermal delivery of natural therapeutics. Nanomedicine (Lond). 2024;19(21-22):1801-19. doi: 10.1080/17435889.2024.2375193, PMID 39056148.
17. Fadaei MS, Fadaei MR, Kheirieh AE, Rahmanian-Devin P, Dabbaghi MM, Nazari Tavallaei K et al. Niosome as a promising tool for increasing the effectiveness of anti-inflammatory compounds. Excli J. 2024 Feb;23:212-63. doi: 10.17179/excli2023-6868, PMID 38487088.
18. Laxmi BV, Bhikshapathi DV, Rajesham VV, Poornima P, Sandhya P, Arjun G. Maximizing the potential of ibrutinib: multi-factor optimization and interaction analysis for improved nanobubble formulation and bioavailability performance. Int J App Pharm. 2025 May;17(5):214-26. doi: 10.22159/IJAP.2025v17i5.54081.
19. Mamatha P, Bhikshapathi DV. Preparation and in-vitro evaluation of pemigatinib nanosponges tablets by box-Behnken design. Int J Pharm Qual Assur. 2023 Sep;14(3):791-800. doi: 10.25258/ijpqa.14.3.56.
20. Ahad A, Aqil M, Kohli K, Sultana Y, Mujeeb M, Ali A. Formulation and optimization of nanotransfersomes using experimental design technique for accentuated transdermal delivery of valsartan. Nanomedicine. 2012;8(2):237-49. doi: 10.1016/j.nano.2011.06.004.
21. Ahad A, Raish M, Al-Mohizea AM, Al-Jenoobi FI, Alam MA. Enhanced anti-inflammatory activity of carbopol loaded meloxicam nanoethosomes gel. Int J Biol Macromol. 2014;67:99-104. doi: 10.1016/j.ijbiomac.2014.03.011, PMID 24657163.
22. Touitou E, Dayan N, Bergelson L, Godin B, Eliaz M. Ethosomes – novel vesicular carriers for enhanced delivery: characterization and skin penetration properties. J Control Release. 2000 Apr;65(3):403-18. doi: 10.1016/S0168-3659(99)00222-9, PMID 10699298.
23. Bendas ER, Tadros MI. Enhanced transdermal delivery of salbutamol sulfate via ethosomes. AAPS PharmSciTech. 2007 Apr;8(4):E107. doi: 10.1208/pt0804107.
24. Song CK, Balakrishnan P, Shim CK, Chung SJ, Chong S, Kim DD. A novel vesicular carrier, transethosome, for enhanced skin delivery of voriconazole: characterization and *in vitro*/*in vivo* evaluation. Colloids Surf B Biointerfaces. 2012;92:299-304. doi: 10.1016/j.colsurfb.2011.12.004. PMID 22205066.
25. Moolakkadath T, Aqil M, Ahad A, Imam SS, Iqbal B, Sultana Y et al. Development of transethosomes formulation for dermal fisetin delivery: box-Behnken design, optimization, *in vitro* skin penetration, vesicles-skin interaction and dermatokinetic studies. Artif Cells Nanomed Biotechnol. 2018;46 sup2:755-65. doi: 10.1080/21691401.2018.1469025.
26. Patel BK, Parikh RH. Formulation development and evaluation of temozolomide-loaded hydrogenated soya phosphatidylcholine liposomes for the treatment of brain cancer. Asian J Pharm Clin Res. 2016 Mar;9(3):340-4.
27. Parvez Baig R, Wais M. Formulation and development of proniosomal gel for topical delivery of amphotericin B. Int J Pharm Pharm Sci. 2022 Jan;14(1):37-49. doi: 10.22159/ijpps.2022v14i1.43237.
28. Md S, Mehboob SZ, Doddayya H. Preparation and characterization of fluconazole topical nanosponge hydrogel. Int J Pharm Pharm Sci. 2024 Apr;16(4):18-26. doi: 10.22159/ijpps.2024v16i4.50589.
29. Reddy MS, Begum Z. Formulation and *in vitro* evaluation of gastro-retentive in situ floating gels of telmisartan cubosomes. Int J Curr Pharm Sci. 2022 Jan;14(1):44-53. doi: 10.22159/ijcpr.2022v14i1.44111.
30. Kumbhar D, Wavikar P, Vavia P. Niosomal gel of lornoxicam for topical delivery: *in vitro* assessment and pharmacodynamic activity. AAPS PharmSciTech. 2013 Sep;14(3):1072-82. doi: 10.1208/s12249-013-9986-5.
31. Polat HK, Ünal S, Aytekin E, Karakuyu NF, Pezik E, Haydar MK et al. Formulation development of lornoxicam loaded heat triggered ocular in-situ gel using factorial design. Drug Dev Ind Pharm. 2023 Sep;49(9):601-15. doi: 10.1080/03639045.2023.2264932, PMID 37788164.

32. Shah H, Nair AB, Shah J, Bharadia P, Al-Dhubiab BE. Proniosomal gel for transdermal delivery of lornoxicam: optimization using factorial design and *in vivo* evaluation in rats. Daru. 2019 Jun;27(1):59-70. doi: 10.1007/s40199-019-00242-x, PMID 30701460.
33. He Y, Majid K, Maqbool M, Hussain T, Yousaf AM, Khan IU et al. Formulation and characterization of lornoxicam-loaded cellulosic-microsponge gel for possible applications in arthritis. Saudi Pharm J. 2020 Aug;28(8):994-1003. doi: 10.1016/j.jsps.2020.06.021. jsps.2020.06.021.
34. Tawfeek HM, Abdellatif AA, Abdel-Aleem JA, Hassan YA, Fathalla D. Transfersomal gel nanocarriers for enhancement the permeation of lornoxicam. J Drug Deliv Sci Technol. 2020;56:101540. doi: 10.1016/j.jddst.2020.101540.
35. Acharya A, Ahmed MG. Rao BD, Vinay CH. Ethosomal gel of lornoxicam. Manipal J PharmSci. 2016 Jan;2(1):13-20. doi: Not available.